

the shift in the resonant frequency of a cavity and the change in the Q-value of a cavity are measured together. When an electron concentration is low ($\eta = ne^2 / m\epsilon_0 \omega^2 \ll 1$), the first order perturbation theory is good, because the plasma does not appreciably disturb the electric field. When a density is increased, the electric field E in the presence of a plasma becomes appreciably different from E_0 in the absence of a plasma. Then the following three effects must be considered.

- (A) drift of a plasma by Lorentz force in the presence of a magnetic field.
- (B) ac space charge (commonly called "plasma resonance" makes itself feel when η approaches unity, so called when the probing frequency approaches and it is equal to the plasma frequency.)
- (C) when both η and the pressure are high enough so that the Q-value is lowered, the overlapping of higher mode also causes E to be different from E_0 .

By proper method of design, the major effects (A) and (B) may be eliminated. (A) As the magnetic field in the z-direction exists in our experimental device, if the distribution of the electric field in a cavity has the electric field E_z only in the direction of a axis, the plasma is not caused to drift by Lorentz force. (B) This can be shown theoretically as follows, by combining Maxwell eq. with continuity eq. and assuming such a harmonic time variations as $\exp(j\omega t)$.

$$-\frac{\partial \rho}{\partial t} = \text{div } i \quad (1) \quad \text{div } E = \rho / \epsilon_0 \quad (2)$$

From (1), $-j\omega\rho = \text{div } \sigma E$

From (2), $\text{div } E = \text{div } \sigma E / (-j\omega\epsilon_0) = \text{div } (1-K) E$; $K = 1 + \sigma/j\omega\epsilon_0$

$$= -\text{grad } K \cdot E + (1-K) \text{div } E$$

$$\therefore \text{div } E = -\text{grad } K \cdot E / K ; K = f(n).$$

The eq. states that ρ will be zero when the applied electric field E is normal to the density gradient. If therefore, by a proper experimental arrangement, this condition is satisfied, the space charge effect will not limit the microwave cavity method from measuring a high electron density. In our experimental device, an electron density varies with radially directional position from a axis ($\text{grad } n \neq 0$). We selected TM_{010} mode from the above reasons. A cylindrical cavity that oscillates in the TM_{010} mode with a cylindrical plasma column placed along the axis of a cavity resonator, satisfies the required condition. Furthermore, TM_{010} mode has large separation with the higher modes¹⁾.

In the presence of a static Magnetic field, a plasma becomes an anisotropic medium. As the result, a plasma conductivity is a tensor function of position and a dielectric coefficient of a plasma is defined by the following tensor²⁾.

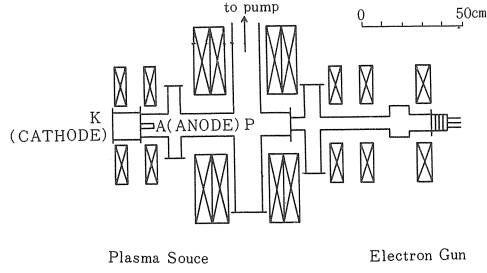


Fig. 1 Schematic diagram of experimental device

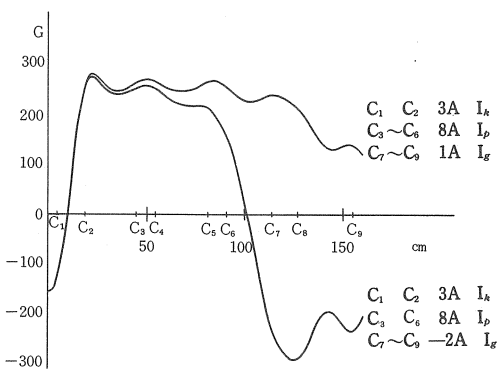


Fig. 2 Magnetic field intensity (theory)

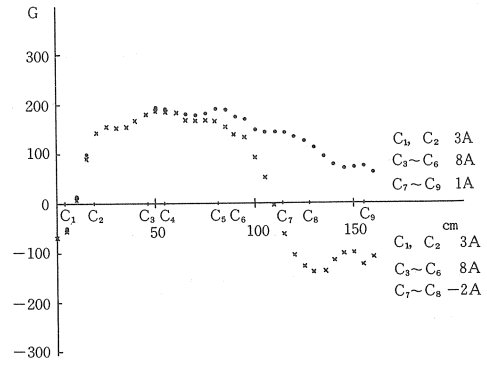


Fig. 3 Magnetic field intensity (experimental value)

$$K = 1 + \sigma / j\omega\epsilon_0 = \begin{bmatrix} K_{rr} & K_{r\theta} & 0 \\ K_{\theta r} & K_{\theta\theta} & 0 \\ 0 & 0 & K_{zz} \end{bmatrix}$$

$$K \text{ is given by } K_{zz} = 1 + \sigma_{zz} / j\omega\epsilon_0 = 1 - \frac{\alpha^2}{(1 - j\gamma)}$$

in the similar fashion

$$K_{\theta\theta} = K_{rr} = 1 - \frac{\alpha^2 (1 - j\gamma)}{(1 - j\gamma)^2 - \beta^2}$$

$$K_{r\theta} = -K_{\theta r} = j \frac{\alpha^2 \beta}{(1 - j\gamma)^2 - \beta^2}$$

where $\alpha^2 = \omega_p^2 / \omega^2$, $\beta = \omega_b / \omega$, $\gamma = \nu_c / \omega$, and $\omega_p^2 = ne^2 / m\epsilon_0$, here n is a electron density, $\omega_b = eB/m$ is a electron cyclotron frequency and ν_c is a electron collision frequency for momentum transfer.

For the TM_{0m0} mode in the Absence of a plasma¹⁾,

$$E_r = E_\theta = H_r = 0$$

$$E_z = J_0(k_1 r) = J_0(x_{0m} r/a)$$

$$H_\theta = -J_0(k_1 r) = -J_0(x_{0m} r/a),$$

where $x_{0m} = m^{th}$ root of $J_0(x) = 0$ and a is the radius of a cavity.

With the plasma present, the axial electric field is given by solving Maxwell eq. as $\text{div } \mathbf{E} = 0$,

$$\frac{d^2 E_z}{dr^2} + \frac{1}{r} \frac{dE_z}{dr} + k^2 K_{zz} E_z = 0 \quad ; \quad 0 \leq r \leq R$$

$$\frac{d^2 E_z}{dr^2} + \frac{1}{r} \frac{dE_z}{dr} + k^2 E_z = 0 \quad ; \quad R \leq r \leq a,$$

where R is the radius of a plasma and $k = \omega/c$; ω is a resonant angular frequency.

The solution of above Maxwell eq. is given by

$$[A] \quad \alpha^2 = \eta < 1, \quad \gamma = 0$$

$$E_z = E_0 J_0(k K_{zz}^{1/2} r) + E' N_0(k K_{zz}^{1/2} r) \quad ; \quad 0 \leq r \leq R \quad (3)$$

$$E_z = A J_0(kr) + B N_0(kr) \quad ; \quad R \leq r \leq a \quad (4)$$

In order to have the finite solution (3), E' becomes zero. The electric field E_z and its derivatives must be continuous at $r = R$ and E_z must vanish at $r = a$. From above-mentioned relations²⁾

$$C = \frac{N_0(ka)}{J_0(ka)} \quad (5)$$

$$\frac{C J_0(kR) + N_0(kR)}{C J_1(kR) + N_1(kR)} = \frac{J_0(k K_{zz}^{1/2} R)}{K_{zz}^{1/2} J_1(k K_{zz}^{1/2} R)} \quad (6)$$

Eq. (6) gives the equation for a resonant frequency.

$$[B] \quad \alpha^2 = \eta \geq 1, \quad \gamma = 0$$

In the similar way as [A],

$$E_z = E_0 I_0(k \sqrt{\alpha^2 - 1} r) \quad ; \quad 0 \leq r \leq R \quad (7)$$

$$E_z = A J_0(kr) + B N_0(kr) \quad ; \quad R \leq r \leq a \quad (8)$$

$$\frac{C J_0(kR) + N_0(kR)}{C J_1(kR) + N_1(kR)} = \frac{I_0(k \sqrt{\alpha^2 - 1} R)}{-\sqrt{\alpha^2 - 1} I_1(R \sqrt{\alpha^2 - 1} R)} \quad (9)$$

So that eq. (9) gives the equation for a resonant frequency, too.

In the limit of vanishing small plasma densities, $K_{zz} = 1$ and eq. (6) properly reduces to $J_0(ka) = 0$, which is the characteristic equation for a empty cavity. Eq. (6), (9) posses an infinite number of modes of TM_{0m0} class. It was solved numerically for its lowest root in terms of a dimensionless quantity ka . The resonant frequency is also given according to the electron density of a plasma. As a result, the relation between the shift in the resonant frequency of a cavity and the electron density is given from eq. (6) and (9).

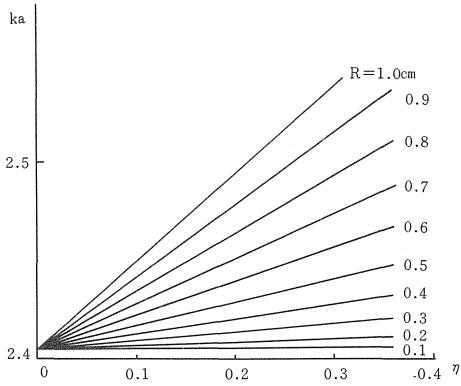


Fig. 4 The relation between Ka and η (1)

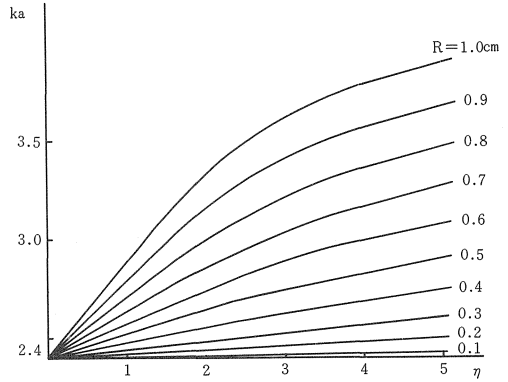


Fig. 5 The relation between Ka and η (2)

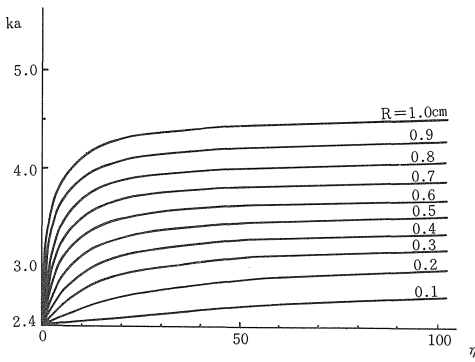


Fig. 6 The relation between Ka and η (3)

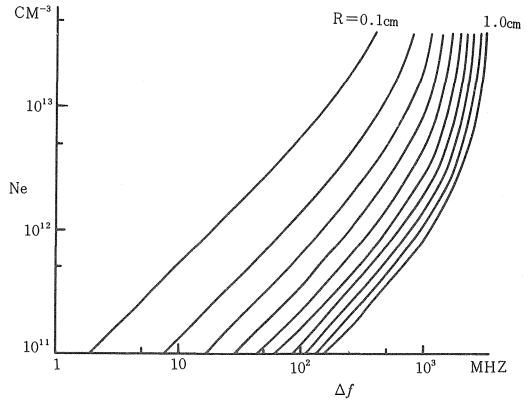


Fig. 7 The relation between Ne and Δf (1)

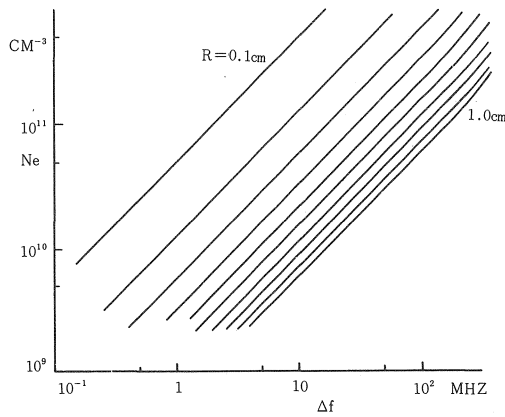


Fig. 8 The relation between Ne and Δf (2)

Then, the relation (6) and (9) are plotted in Fig.4~6 and the radius of a plasma is put as a parameter, so-called plotted the resonant frequency of a $TM_{0,10}$ mode cylindrical cavity as the function of the electron density of an axially located plasma, and in Fig. (7), (8) is plotted the electron density as the function of the shift in MHz unit of the resonant frequency of a $TM_{0,10}$ mode, where the radius of a cylindrical cavity is 2.98 cm.

3. Probe theory in the presence of a magnetic field

The electron concentration of a plasma is got from the electron current near the space potential.

In the case of a plane probe, it can be shown that the number of electrons striking 1 cm^2 per second of a solid plane parallel to a magnetic field B decreases as B rises, and the electron current near the space potential is given by the following equation³⁾,

$$\frac{j}{e} = \frac{nv}{4} \frac{8 + (\omega\tau)^2 \{1 - \exp(-2\pi/\omega\tau)\}}{2 \{4 + (\omega\tau)^2\}},$$

where j is a current density near the space potential, e is a charge of electron, τ is a mean collision time, v is a mean radon velocity $\sqrt{3kT_e/m}$ (m is an electron mass and T_e is an electron temperature), and ω is a cyclotron angular frequency.

The magnitude of a electron current near the space potential is given by Bohm, Burhop, and Massey for a probe of arbitrary shape⁴⁾,

$$\frac{j}{e} = \frac{nv}{4} \left(K + \frac{Sv}{16\pi\sqrt{\alpha}CD} \right)^{-1},$$

where K is a constant ($K = 1$), S is a probe surface area, $\alpha = D_{\perp}/D = 1/(1 + \omega^2\tau^2)$, $D = \lambda v/3$, λ is a mean free path along a magnetic field, C is a capacity of probe, and D_{\perp} is a diffusion coefficient along and across the field. In the case of a spherical probe,

$$\begin{aligned} b &= a + r_L \approx a \\ d &= \sqrt{\alpha} (a + \lambda) \approx \sqrt{\alpha\lambda}, \end{aligned}$$

where a is the radius of a spherical probe and r_L is Lamor radius. And

$$C = \frac{d(1-p^2)^{1/2}}{\tanh^{-1}(1-p^2)^{1/2}} ; p = \frac{b}{d} \leq 1$$

$$C = \frac{d(p^2-1)^{1/2}}{\tan^{-1}(p^2-1)^{1/2}} ; p = \frac{b}{d} \geq 1.$$

These formulas give the saturation electron current at a small positive potential under the assumption that $T_i \ll T_e$, that orbital motions can be neglected in the free - fall region, and that quasi-neutrality obtains elsewhere.

4. Experimental apparatus

The experimental apparatus used now is schematically shown in Fig.1. A plasma generated by the plasma source placed at the left end flows into a vacuum chamber through the hollow anode of the plasma source and the vacuum chamber is made of Pyrex glass.

Solenoidal coils placed outside the vacuum chamber produce *d.c.* magnetic field. The intensity of the magnetic field is varied from 0 to 600 Gauss.

Helium gas is supplied into the central region of the vacuum chamber from a gas bombe through a leak valve in the left end. The pressure of the arrangement is varied in the range from 10^{-5} to 10^{-1} Torr and the lowest attainable pressure is in the range of 10^{-6} Torr.

The magnetic field intensity as the function of a position along the linear machine is shown in Fig.2 (theoretical value), where $C_1 \sim C_9$ denote the positions of coils. And Fig.3 denotes the experimental value of the magnetic field intensity in our experimental device.

The cylindrical cavity is made of brass. We made holes on the axis of it and covered these holes with wire net. The wire net arrests the lowering of the Q-value. We put the cavity at *P* in the vacuum chamber, then the beam plasma passes through the cavity. The shift of the resonant frequency of cavity is measured by a spectrum analyser.

5. Experimental results

The radial density variation in a plasma column is measured by a radially movable probe at *P* in the vacuum chamber, whose width of a half value is about 2 cm in spite of the kind of probe used in the measurement.

The probes used are disk, plane, spherical and cylindrical probe. Each probe is

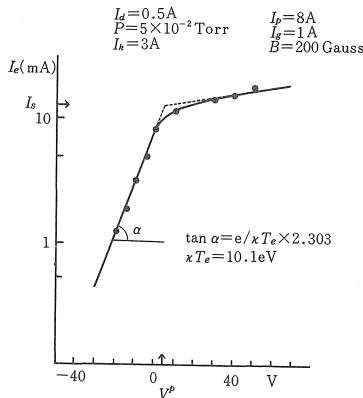


Fig.9 Probe characteristic (spherical probe)

consisted of a tungsten electrode and a tungsten wire (0.5 mm diameter) and the tungsten wires are all sheathed in glass. The radius of the disk probe is 1 mm and the thickness of it is 0.5 mm. The plane probe is sheathed by a glass except for the circular part of the disk probe and the radius of it is 1 mm. The radius of the spherical probe is 1 mm. The cylindrical probe is made of tungsten wire and the radius of the electrode is 0.5 mm and the length of it is 1 mm.

We measured probe characteristics by using a X-Y recorder or a synchroscope, but we mainly used a X-Y recorder. One example of a probe characteristic is shown in Fig.9. I_e is electron current. Electron temperatures κT_e are about $10eV$ in spite of the kind of probe from probe characteristics. Space potential V_p are about $5V$ in these probes.

The radius of a cylindrical cavity is $a = 2.98\text{ cm}$ and the length of it is $L = 5.00\text{ cm}$, so that the resonant frequency of a cavity is 3.84 GHz . The microwave cavity method gives information averaged over the radius of a plasma $R = 1.5\text{ mm}$. We put in the input to a cylindrical cavity by a rod antenna and received the output by a rod antenna too. We set both of them symmetrically at $r = 1\text{ cm}$ points from the central point.

The effect of a magnetic field or a discharge current I_d or a Helium gas pressure for measured electron densities is shown in Fig.10, Fig.11, and Fig.12. Here, a cylindrical probe is plotted without taking account of the effect of a magnetic field.

In the first place, an electron concentration versus a discharge current I_d is shown in Fig.10. The microwave cavity method and the probe method agree within the experimental errors in spite of the form of an electrode besides the cylindrical probe, where $P = 5 \times 10^{-2}\text{ Torr}$ and $B = 200\text{ Gauss}$.

In Fig.11, an electron density versus a magnetic field is shown. The probes are in

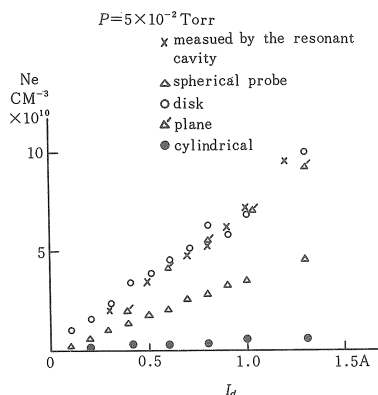


Fig. 10 Electron density versus discharge current

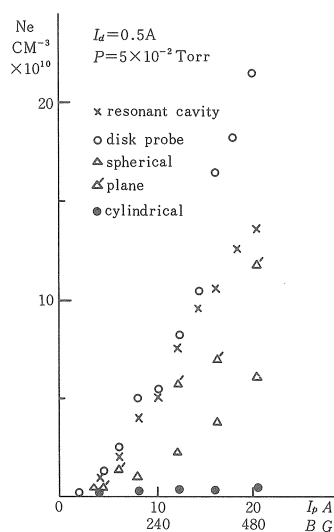


Fig. 11 Electron density versus magnetic field

agreement with the microwave cavity method in the region where $B \leq 480$ Gauss within the experimental errors besides the cylindrical probe, so that the probe theory in a magnetic field holds in the region of this measurement where $P = 5 \times 10^{-2}$ Torr and $I_a = 0.5A.$.

Fig.12 shows the relation of an electron density versus a Helium gas pressure at a particular condition. The spherical probe is in agreement with the microwave cavity method within the experimental errors through the whole region of pressure. But the plane probe fairly differs from the microwave cavity method in the region from 2×10^{-4} to 10^{-2} Torr. On the contrary, in the region from 10^{-2} to 10^{-1} Torr the probe theory in a magnetic field holds in spite of the shape of an electrode. The cylindrical probe gives a very smaller electron density than that measured by the microwave cavity method as a matter of course, because the effect of a magnetic field is not taken

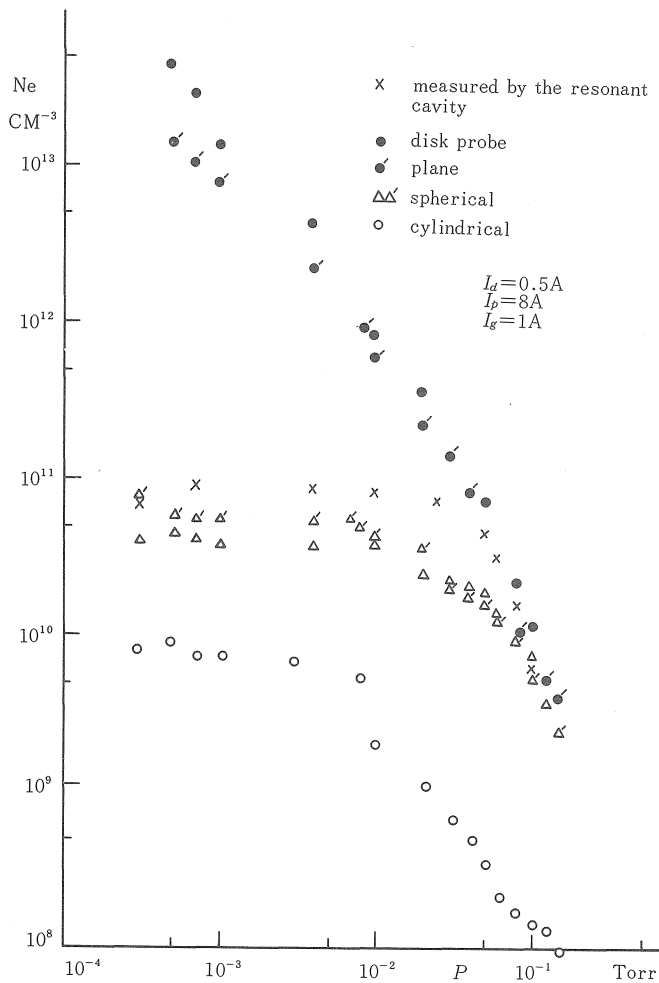


Fig. 12 Electron density versus pressure

account of.

As the result of trying a cross check by the microwave cavity method, a spherical probe is in relatively good agreement with the microwave cavity method and so the probe theory for a spherical probe in a magnetic field holds though this probe theory neglects electric fields and orbital motions and is valid only for $\kappa T_e \gg \kappa T_i$. Also the theory of a plane probe in a magnetic field which is derived for an infinite plane probe is not strictly applicable.

6. Conclusions

We compare the electron densities measured by the disk, plane, spherical, and cylindrical probe with that measured by the microwave cavity method. Cylindrical probe gives a very smaller electron density than that measured by the microwave cavity method as is expected, because the effect of a magnetic field is not taken account of. The probes besides a cylindrical probe agree with the cavity method in spite of the strength of a magnetic field ($B \leq 480$ Gauss) in the ceration region of the higher Helium gas pressure. But when we compare the electron densities in the wide region of Helium gass pressure, only the spherical probe agrees with the cavity method. Therefore, it becomes evident that the theory of a spherical probe in a magnetic field gives us the most confidence.

References

- 1) C.G. Montgomery, Technique of Microwave Measurement, Massachusetts Institute of Technology, Radiation Laboratory series 11 (MacGraw-Hill Book Company, Inc., 1947) P.298-P.299.
- 2) S.J. Buchsbaum, L. Hower, and S.C. Brown, The Physics of Fluids 3 (1960) 806.
- 3) R.J. Rickerton and A. Von Engel, Proc. Phys. Soc. (London) B 69 (1955) 468.
- 4) F.F. Chen, Plasma Diagnostic Techniques ed. by R.H. Huddlestone, and S.L. Leonard (Academic Press, New York, 1965) P.164.